Energy Conversion and Management 74 (2013) 462–470

Contents lists available at SciVerse ScienceDirect

Energy Conversion and Management

journal homepage: www.elsevier.com/locate/enconman

The impact of biomass co-combustion on the erosion of boiler convection surfaces

Marek Pronobis, Wacław Wojnar *

Silesian University of Technology, Faculty of Energy and Environmental Engineering, Institute of Power Engineering and Turbomachinery, Division of Boilers and Steam Generators, Konarskiego 20, 44-100 Gliwice, Poland

ARTICLE INFO

Article history:
Received 13 November 2012
Accepted 28 June 2013
Available online 29 July 2013

Keywords:
Steam boilers
Exfoliation
Oxide layers
Erosion

ABSTRACT

The erosive wear of boiler tubes caused by fly ash in coal combustion flue gases has been studied for a long time. However, there are practically no data concerning the intensity of the erosion of the heating surfaces of boilers fired with both coal and biomass, and thus it is difficult to design these particular areas appropriately.

The essential problem is the tendency of the fly ash from biomass combustion to produce ash deposits on the boiler convection surfaces and to cause slagging on the radiant surfaces. In such cases, both an increase in the deposits and a shortening of the time over which the ash fouling accumulates to the maximum level are observed. Consequently, if the boiler is fitted with steam or air blowers, they are started more frequently; if not, they have to be installed. The research conducted here proves that the situation leads to serious damage to the tubes, which results from the erosion caused by ash particles carried by the blowing agent jet.

The authors of this paper attempt to make a quantitative evaluation of the impact of co-firing two types of biomass (coniferous wood chips and willow wood chips) on both types of tube erosion.

© 2013 Elsevier Ltd. All rights reserved.

1. Introduction

The main threat to the reliability of biomass co-firing boilers is a high-temperature corrosion [1,2]. However, in some cases, co-firing may also have a significant effect on the fly ash erosion.

Erosive damage to convection surfaces is mainly observed in pulverised fuel boilers, where most of the ash, together with flue gas streams, flows through heat exchange areas.

In result of erosion the thickness of boiler tubes decreases leading eventually to their rupture. The standard method of tube thickness identification is the ultrasonic inspection. The gauges used have the resolution of ca. 0.1 mm.

The rate of erosion and the velocity of the particles (usually considered to be identical to the carrier gas velocity) are related by an exponential dependence [3–8]. In [4,8], the exponent values determined experimentally by various researchers are compared. They vary from 2.4 to 3.5 for metal and approximately 3 for ceramic materials to approximately 5 for polymers. The velocity exponent depends on other parameters as well, such as the size and shape of the eroding particles. The value of the exponent mentioned above also depends on the striking angle; in [9], values lower than 2 (1.4–1.6) are given for steel at perpendicular impingement. The exponent value is dependent on the method used to determine the amount of the solid phase involved in the process [10]; using the concentration μ (kg/m^3) (e.g., in [6,7]), the exponent value must be 1 higher than the exponent value found using the erodent mass flow density (kg/m^{2}s) (e.g. [11]). Numerous standard measurements of the erosion of tubes in boilers confirm that the exponent 3.0 (using concentration) may be assumed to be reliable.

At small values of the solid phase concentration in gas, the rate of metal erosion is proportional to the concentration. At high concentration values, the effect of this parameter may be imperceptible [11]).

The rate of erosion-related loss increases as the particle size grows [12], but it is generally assumed that erosion arises if $d_p > 30$ μm, whereas particles with a smaller diameter (typical of biofuel combustion ash) tend to produce ash deposits. Some studies indicate that the impact of d_p decreases above the limit of 50–100 μm, but, in [13], the greatest erosion occurred at $d_p = 1000$ μm. The erosion is also affected by the particle shape. For metal, the greatest erosion occurs for non-spherical particles with sharp edges. Another factor that affects erosion is the erodent particle hardness.

The formation of ash deposits and tube erosion are in opposition to each other. Whenever deposits are formed, erosion does not occur, and vice versa; with erosion, there are no deposits. The factors that determine which of the two phenomena occur

---

* Corresponding author. Tel.: +48 322372374.
E-mail address: waclaw.wojnar@polsl.pl (W. Wojnar).

0196-8904/$ - see front matter © 2013 Elsevier Ltd. All rights reserved.
http://dx.doi.org/10.1016/j.enconman.2013.06.059

Nomenclature

A^r	ash content in the fuel (as-received state), %
D	outer tube diameter, m
d_b	blower nozzle diameter, m
d_p	particle diameter, μm
c_m, c'_m	indices characterising the ash composition
c_{pl}	mean fly ash concentration in the flue gases, g/m^3
CWB	coniferous wood biomass
e_e	erosion coefficient defining the erosive properties of the fly ash, μm/h
ECO	economiser
EMM	the external mineral matter of the biomass
F_b	blower nozzle cross-section, m^2
HC	hard coal
i	enthalpy, kJ/kg
IMM	internal mineral matter of the biomass
k	heat transfer coefficient, W/m^2 K
$m_{st\ b}$	steam mass per 1 blowing cycle, kg
$\dot{m}_{st\ b}$	steam mass flow from the blower, kg/s
n	number of blower starts per 24 h
Q_i^r	lower calorific value, kJ/kg
p	steam pressure at the blower inlet, bar
p_L	steam pressure at the blower nozzle outlet, bar
p_{ap}	ambient pressure, bar
R	blower effective radius [15], mm
RAH	regenerative air preheater
$R_{0.03}$	content of fly ash grains larger than 30 μm, %
s	entropy, kJ/kg K
SH	superheater
S^r	sulphur content in the fuel (as-received state), %
T_{fg}^m	mean flue gas temperature in the bank, K
y	distance from the blower nozzle outlet, m
$v_e=\Delta h/\tau$	erosion rate, μm/h
$v_{e\ b}$	blower operation-related erosion rate (calculated according to formula (1)), μm/h
v_b	blower travel rate, mm/s,
w	steam flow velocity in the blower lance, m/s
w_2	blowing agent velocity outside the nozzle, m/s
w_L	steam velocity at the blower nozzle outlet, m/s
w_{max}	maximum velocity of the dust-laden flue gases in the duct section, m/s
w_o	mean flue gas velocity in the empty duct at the bank inlet, m/s
w_{fg}	mean flue gas velocity in the free section of the tube bank, m/s
W_t^r	moisture content in the fuel (as-received state), %
WWC	willow wood chips
Y_D	mass content of co-fired biomass, %
Z_D	power share of co-fired biomass, %

Greek symbols

β_w	parameter defining the flue gas velocity distribution in the boiler duct
β_c	parameter defining the fly ash concentration distribution in the flue gases
β_m	parameter defining the impact of the operating temperature and the steel grade on the erosive wear
β_2	parameter defining the impact of longitudinal pitch of the bank on the erosive wear of the tubes
Δh	thickness loss of the tube, μm, mm
ρ_L	steam density at the blower nozzle outlet, kg/m^3
$\sigma_1 = s_1/D$	relative transverse pitch of the tube, m
$\sigma_2 = s_2/D$	relative longitudinal pitch of the tube, m
τ_∞	rise time of ash deposits (the time for the fouling to reach the maximum), h
$\tau_{nb\ a}$	annual time with the blower shut down, h/a
$\tau_{c\ b}$	blowing cycle duration time, s
τ_a	annual boiler operating time, h/a
$\tau_{b\ a}$	annual duration time of the erosion process caused by ash blowing, h/a
τ_{b_1}	unit time of the coil exposure to erosion in one blower operation cycle, s
η_p	mean probability of ash particle impingement on the tube
Ψ_z	thermal efficiency of a tube bank

are the size of the fly ash particles, their composition and the flue gas velocity.

The mean velocity of ash particles in the boiler convection banks can reach up to 8–12 m/s. The local velocity of ash in flue gases is higher when the particles of ash pass between the tubes and the boiler walls, where the local velocity can reach up to 40 m/s [7].

Research on the erosive wear of boiler tubes caused by fly ash began in the 1950s [6] and continued later [7,8,10,14] for coal combustion ash, peat and sand ash. However, there are practically no reference data concerning the intensity of the erosion of the heating surfaces of boilers co-fired with coal and biomass, and thus it is difficult to design these particular areas appropriately.

There are numerous works in the reference literature that are devoted to the problem of damage done to tubes by fly ash carried by flue gases. Only recently, however, was research conducted on erosion depending on the operation of ash blowers fed with steam or air [15]. Given the significant impact of biofuel co-firing on the fouling of the boiler heating surfaces, this paper attempts to analyse the dependence between this phenomenon and the erosion resulting from the higher frequency of the starts of the jet blowers.

Swirski's dependence is typically used in the Polish literature [7]. According to this dependence, the amount of tube material erosion over time (erosion rate) (μm/h) may be expressed as

$$\Delta h/\tau = v_e = 2.33\times10^{-7} w_o^3 \beta_w^3 e_e c_{pl} \beta_c \beta_m \beta_2 \eta_p \qquad (1)$$

The value of η_p (the mean probability of ash particle impingement on the tube) depends on the particle size of the fly ash. Due to the lack of data concerning the particle size distribution of fly ash resulting from the co-firing of biomass with coal, the calculations were performed by assuming monodisperse fly ash with a particle diameter of d_p = 45 μm. This size represents an average value of the diameter of fly ash particles in Polish pulverised fuel boilers.

Dependence (1) describes the loss of material of the steel tubes at points with maximum erosion, which corresponds to an angle of approximately 40° to the axis of the dust-laden gas stream. The method of calculating the individual elements of the formula are given in [3].

The ash erosion coefficient e_e (μm/h) [7] is determined empirically on a purpose-built test unit and is equal to material loss for an angular coordinate of ϕ = 45°, a velocity of w_o = 35 m/s and a fly ash concentration of c_{pl} = 100 g/m^3. The results of the erosion coefficient testing conducted in [7] imply that the value of e_e is most affected by the chemical composition of the ash defined by the coefficient c'_m in the following equation:

$$c'_m = \frac{Fe_2O_3}{SiO_2 + Al_2O_3} \qquad (2)$$

However, the reference literature includes studies that prove that the erosion intensity is also a different function of the fly ash composition; [16] presents a chart that indicates that the erosion increases with an increase in the coefficient (SiO_2–$2Al_2O_3$). This coefficient reflects the contents of highly erosive minerals based on silicon oxide (quartz, chalcedony) and, much less dangerous in this respect, aluminosilicates (e.g., kaolinite $Al_4(OH)_8Si_4O_{10}$).

Another problem is the tendency of the biomass combustion fly ash to produce ash deposits on the boiler convection surfaces and to cause slagging on the radiant surfaces [17–19]. In these cases, both an increase in the amount of material deposited and a shortening of the duration during which the ash fouling accumulates to the maximum level are observed [20]. Consequently, if the boiler is fitted with blowers, they are started more frequently; if not, they have to be installed. Previous research [15] demonstrated that the situation leads to serious damage to the tubes, which results from the erosion caused by ash particles carried by the blowing agent jet.

The authors of this paper attempt to evaluate the impact of biomass co-firing on both types of tube erosion (fly ash erosion and erosion caused by steam jet ash blowers) quantitatively.

2. Example calculations of erosion caused by fly ash carried by flue gases

2.1. Co-firing of coniferous wood biomass – CWB

To evaluate the impact of biomass co-firing on the erosion hazard to convection surfaces, calculations are performed for the OP 230 boiler by assuming the fuel characteristics listed in Table 1 (hard coal – HC, coniferous wood biomass – CWB, and their mixtures). Coal given in Table 1 and Table 4 is a typical Upper Silesian coal which is burned in the Polish power plants. The properties of CWB correspond to the average for the supply of one of the domestic power plants.

The 0-dimensional thermal calculations of the boiler were carried out according to procedures [19,22,23].

The biomass thermal fractions Z_D in the fuel mixture are assumed to be the basic quantity parameter; hence, the following variants are calculated:

HC variant – $Z_D = 0$ (combustion of pulverised coal only).
CWB_10 variant – $Z_D = 10\%$.
CWB_20 variant – $Z_D = 20\%$.
CWB_50 variant – $Z_D = 50\%$.

Based on these percentages, the mass fractions Y_D corresponding to the respective thermal fractions are determined. It is assumed that the biomass is fed into the pulverised fuel ducts before the burners, i.e., a change in its fraction does not affect the location of the flame zone, where the highest temperatures occur in the furnace.

For the CWB fractions given above, the fly ash composition and the changes in the chemical composition and the corresponding values of the parameter c_m and the efficiency level Ψ_z, which defines the impact of fly ash deposits on the heat transfer coefficient on convection surfaces, are determined.

For the purposes of this paper, CWB with a relatively high content of moisture and ash, which is typically used in one of the Polish power plants, is considered. The typical characteristics to be analysed are listed in Table 2, which also presents, for comparative purposes, the composition of the average ash from the combustion of the coal mined in Upper Silesia. The last column presents the value of the coefficient c_m (Basic/Acidic), which is often assumed to be a parameter that characterises the tendency of the fly ash to form deposits:

$$c_m = \frac{Fe_2O_3 + CaO + MgO + Na_2O + K_2O + P_2O_5}{SiO_2 + Al_2O_3 + TiO_2} \tag{3}$$

The introduction of additional biomass fuel results in a change in the chemical composition and the stream of the flue gases, which, consequently, change their radiation properties (emissivity and absorptivity), their velocity and their viscosity, which affect the convective heat transfer intensity.

The co-firing-related change in the amount and the properties of the particles carried by the flue gases leads to a change in the flue gas emissivity and, moreover, in the intensity of the ash fouling of the heating surfaces. The combustion of fuels with characteristics different than the design fuels may cause significant changes in the size and nature of the fouling of the heating surfaces, which in turn has a powerful impact on the amount of heat absorbed by individual areas.

One of the measures of the impact of deposits on the heat transfer is the thermal efficiency Ψz, which is the ratio of the heat transfer coefficients of the tube bank with and without fouling.

$$\Psi_z = \frac{k_z}{k_c} \tag{4}$$

Papers [17,22] give formulae to calculate the thermal efficiency of surfaces covered with loose or partially sintered deposits. For fly ash carried by flue gases, coal and biomass co-firing results in an increased value of c_m. Consequently, the efficiency of the boiler heating surfaces (assuming a mean exponent for in-line and staggered banks) varies according to

$$\frac{\Psi_{z\Sigma}}{\Psi_{zW}} = \left(\frac{c_{m\Sigma}}{c_{mW}}\right)^{-0.354} \tag{5}$$

which proves that the value of Ψ_z decreases as the biomass content increases. A further decrease in Ψ_z, though difficult to assess, may also be caused if fine granulated components are fed into the fly ash (leading to a decrease in $R_{0.03}$), which results from the condensation and the solidification of volatile mineral fractions. This phenomenon may be of significant importance for fuels with a high content of sodium and potassium. A decrease in the thermal efficiency of the heat exchangers results in a decrease in the boiler efficiency due to an increase of the exit flue gas temperature.

With the use of a regenerative air preheater (RAH), an increase in fouling results in an increase in the consumption of energy

Table 1
Characteristics of the fuels assumed for the calculations.

	Z_D (–)	Y_D (–)	N^r (%)	C^r (%)	S^r (%)	H^r (%)	Cl^r (%)	O^r (%)	W_t^r (%)	A^r (%)	Q_i^r (kJ/kg)
HC[a]	0	0	0.91	54.41	0.66	3.44	0.22	8.0	9.67	22.69	21034
CWB[a]	1.0	1.0	0.14	22.26	0.11	2.70	0.01	11.58	52.42	10.78	6295
HC + CWB[b]	0.10	0.271	0.70	45.71	0.51	3.24	0.16	8.97	21.24	19.47	17,043
	0.20	0.455	0.56	39.78	0.41	3.10	0.12	9.63	29.13	17.27	14,326
	0.50	0.77	0.32	29.67	0.24	2.87	0.06	10.75	42.57	13.52	9690

[a] HC – hard coal.
[b] CWB – coniferous wood biomass.

Table 2
Chemical composition of ash from the combustion of HC, CWB, and their mixtures.

Fuel	CaO (%)	MgO (%)	Fe_2O_3 (%)	Na_2O (%)	K_2O (%)	SiO_2 (%)	Al_2O_3 (%)	P_2O_5 (%)	TiO_2 (%)	c_m	$\frac{\Psi_{z\Sigma}}{\Psi_{zW}}$[a])
HC	3.50	3.50	9.00	0.80	2.50	60.00	19.70	0.1	0.90	0.24	0.24
CWB [21]	18.13	2.26	3.56	0.39	3.24	63.02	7.90	1.12	0.38	0.40	0.83
Z_D = 0.10	5.69	3.31	8.18	0.74	2.61	60.45	17.93	0.25	0.82	0.26	0.97
Z_D = 0.20	7.66	3.15	7.45	0.68	2.71	60.86	16.35	0.39	0.75	0.28	0.95
Z_D = 0.50	12.48	2.74	5.66	0.55	2.95	61.85	12.46	0.73	0.58	0.34	0.88

[a] Σ – for coal – biomass mix combustion; *W* – for coal combustion.

required to cause agents to flow and causes a decrease in the preheated air temperature. The higher consumption of energy required to pump agents is caused by an increase in the flow resistance in the preheater and greater leakage of air into the flue gases. The basic heat exchange mechanism in the RAH remains practically unaffected if the heating elements become covered with a layer of deposits with a low heat conductivity, which is proved by the fact that the efficiency of both uncoated and enamelled metal plates is practically the same [24]. In addition, a reduction in the heating area due to the clogging of some parts of these elements is usually compensated for by a higher intensity of the heat transfer at places where the agents now flow faster.

Due to the difficulties mentioned above related to the evaluation of the changes in the heat flow resistance in the RAH and the lack of data concerning the impact of wood biomass co-firing on the fouling of the furnace and the SH II platens, only the changes in Ψ_z, according to Table 2 are considered, assuming that the boiler is not fitted with a system to remove ash deposits from surfaces. Another simplification is the assumption of monodisperse fly ash with a particle diameter of $d_p = 45$ μm.

The calculation results are listed in Table 3. The erosion rate increases significantly (by a factor of almost 4) as the content of CWB co-fired with coal increases. The biomass assumed for the calculations does feature a relatively high value of ash content, but this ash is a mixture of the internal mineral matter contained in wood and external matter with a high content of SiO_2 (most likely sand), which was mixed with the CWB in the process of preparation. Therefore, this ash does not increase the c_m ratio substantially (from 0.24 for HC to 0.4 for CWB), and thus it does not worsen the fouling of the surfaces as much as other types of biomass with more adverse characteristics could. The significant increment in the flue gas velocity related to the high content of water in the CWB and the relatively low value of c'_m according to formula (2), which slightly increases the erosion index, lead to a substantial increase in the erosion rate.

2.2. Co-combustion of willow wood chips – WWC

To evaluate the impact of the co-fired biomass characteristics on the erosion hazard to the boiler convection surfaces, calculations are performed by replacing the CWB with willow wood chips (WWC). The fuel characteristics are listed in Table 4 (hard coal – HC, willow wood chips – WWC, and their mixtures). The properties of WWC correspond to the average for the supply of one of the

Table 3
Boiler OP 230 calculation results for CWB co-firing (boiler with no ash blowing).

Parameter	HC Z_D = 0	CWB_10 Z_D = 0.1	CWB_20.2 Z_D = 0	CWB_50 Z_D = 0.5
Max. continuous rating (t/h)	230	230	230	230
Steam pressure (MPa)	9.5	9.5	9.5	9.5
Feed water temperature (°C)	185	185	185	185
Spray water mass flow (kg/h)	18,270	21,672	24,624	30,564
Fuel				
Lower calorific value (kJ/kg)	21,034	17,043	14,326	9690
Ash content (%)	22.69	19.47	17.27	13.52
Moisture content (%)	9.67	21.24	29.13	42.57
Steam temperatures (°C)				
At the superheater I stage (SH I) inlet	317	317	317	317
At the superheater III stage (SH III) outlet	540	540	540	540
Flue gas temperatures (°C)				
At the combustion chamber outlet	1230	1218	1205	1155
Before the economiser (ECO)	538	550	562	587
Before the air preheater	349	359	371	395
At the boiler outlet	130	139	148	172
Air temperatures (°C)				
At the preheater inlet	25	25	25	25
At the preheater outlet	297	308	320	345
Boiler efficiency (%)	90.98	90.06	89.06	85.98
Fuel consumption (kg/h)				
HC	32,311	29,380	26,408	17,102
CWB	0	10,907	22,059	57,143
Ash concentration in the ECO (g/m^3)	8.20	8.11	8.03	7.85
Flue gas velocity before the ECO (m/s)	6.22	6.74	7.27	8.92
c'_m index – formula (2) (–)	0.1129	0.1044	0.0966	0.0762
Mean fly ash diameter (μm)	45	45	45	45
Maximum annual erosion loss (mm/a)	0.0255	0.034	0.0448	0.0966

Table 4

The characteristics of the fuels assumed for the calculations.

	Z_D (–)	Y_D (–)	N^r (%)	C^r (%)	S^r (%)	H^r (%)	Cl^r (%)	O^r (%)	W_t^r (%)	A^r (%)	Q_i^r (kJ/kg)
HC[a]	0	0	0.91	54.41	0.66	3.44	0.219	8.0	9.67	22.69	21,034
WWC[b]	1.0	1.0	0.14	42.87	0.05	4.96	0.0	35.72	13.40	2.90	15,128
HC + WWC	0.10	0.134	0.81	52.87	0.58	3.64	0.18	11.71	10.17	20.04	20,244
	0.20	0.258	0.71	51.43	0.50	3.83	0.16	15.15	10.63	17.59	19,511
	0.50	0.582	0.46	47.69	0.31	4.31	0.08	24.13	11.84	11.18	17,599

[a] HC – hard coal.

[b] WWC – willow wood chips.

Table 5

The chemical composition of the ash from the combustion of HC, WWC, and their mixtures.

Fuel	CaO (%)	MgO (%)	Fe_2O_3 (%)	Na_2O (%)	K_2O (%)	SiO_2 (%)	Al_2O_3 (%)	P_2O_5 (%)	TiO_2 (%)	c_m	$\frac{\Psi_{z\Sigma}}{\Psi_{zW}}$[a]
HC	3.50	3.50	9.00	0.80	2.50	60.00	19.70	0.1	0.90	0.24	0.24
WWC [25]	29.99	1.52	7.64	0.40	6.76	42.10	6.11	5.22	0.26	1.06	0.59
Z_D = 0.10	4.02	3.46	8.97	0.79	2.58	59.65	19.44	0.20	0.89	0.25	0.99
Z_D = 0.20	4.63	3.42	8.94	0.78	2.68	59.24	19.12	0.32	0.87	0.26	0.97
Z_D = 0.50	7.50	3.20	8.79	0.74	3.14	57.30	17.65	0.87	0.81	0.32	0.90

[a] Σ – for coal – biomass mix combustion; W – for coal combustion.

domestic power plants. Table 5 presents the respective ash compositions.

The calculation results are given in Table 6. Column one repeats the results for the HC variant – combustion of hard coal only; column two presents the results for the variant WWC 20 (for Z_D = 20%). A decrease in the erosion rate can be observed for co-firing with coal and willow wood chips. This type of biomass features a relatively low content of ash and moisture and a relatively high lower calorific value. Although this ash has a distinctly higher c_m ratio (0.24 for HC and 1.063 for WWC), it does not increase the level of surface fouling significantly with a low content of the WWC ash in the mixture. The decrease in the ash concentration, together with a slight increase in the flue gas velocity and a certain increase in the c'_m index, reduces the erosion loss slightly.

In summary, the following conclusions may be drawn from the calculations of the erosion caused by the fly ash carried by flue gases:

The co-combustion of coal and very moist types of biomass with a relatively high content of ash containing significant proportions of strongly erosive components (SiO_2, Al_2O_3, TiO_2) increases the erosion rate compared to the erosion rate observed for coal combustion only.

The co-combustion of relatively dry biofuels (for example, willow wood chips) with a relatively low content of ash results in a slightly reduced erosion rate compared to the erosion rate observed for coal combustion only.

Thus, the co-combustion of very moist types of biomass should be avoided, especially if the ash contained in them features adverse characteristics from the point of view of the erosion hazard. Such biofuels should be pre-dried or subjected to torrefaction for example. It is also beneficial to gasify such types of biomass in a separate facility, especially because this technology also makes it possible to separate the biomass ash, which can later be disposed of as fertiliser, for example.

3. Evaluation of the erosion hazards caused by more frequents starts of steam jet ash blowers

3.1. Rise time of ash deposits

In [20], the following dependence is developed to define the rise time of ash deposits (the time for the fouling to reach the maximum height) τ_∞ (h):

$$\tau_\infty = 9.01\sigma_2^{-1.723} w_{fg}^{0.744} \left(\frac{R_{0.03}}{24.5}\right)^{0.319} \left(\frac{T_{fg}^m}{373}\right)^{0.249} \tag{6}$$

In this formula, there is no variable characterising the chemical composition of the fly ash, such as c_m, for example. The hard coal ash studied in [22] features values of c_m = 0.176–0.522, which are lower than those for willow wood chips ash according to Table 5. However, both the ash resulting from CWB combustion and all of the ash mixtures obtained in the co-firing of both CWB and WWC have values of c_m that are within the range for which formula (6) remains valid. Therefore, it may be assumed that no significant errors will arise if the following analysis is based on this dependence.

When neglecting the technical parameter of the tube pitch in the bank, it is the flue gas velocity that has the greatest impact on τ_∞. The greater the velocity, the longer the time required for the fouling to reach the maximum height. The lengthening of the rise time of the ash deposits also results from the thickening of the fly ash size and the increase in the flue gas temperature.

By converting formula (6) to a form that allows the evaluation of the change in τ_∞ at biomass co-combustion, the following formula is obtained:

$$\frac{\tau_{\infty\Sigma}}{\tau_{\infty W}} = \left(\frac{w_{fg\Sigma}}{w_{fgW}}\right)^{0.744} \left(\frac{R_{0.03\Sigma}}{R_{0.03W}}\right)^{0.319} \left(\frac{T_{fg\Sigma}^m}{T_{fgW}^m}\right)^{0.249} \tag{7}$$

where “W” and “Σ” relate to coal combustion, which is treated as the reference case, and to biomass - coal co-combustion, respectively.

It is very difficult to generalise the evaluation of the change in $R_{0.03}$ resulting from biomass co-combustion. The ash fed into the boiler together with biofuels is a mixture of the internal mineral matter (IMM) of the biomass and the external mineral matter (EMM) mixed with the biomass in the process of preparation. Because IMM constitutes only a small volume of the biomass matter (approximately 1%), the combustion of pulverised biomass leads to fine-grained ash, which is almost entirely composed of particles smaller than 30 μm, prone to form deposits in the power boiler. The chemical composition and the structure of the ash may be determined by means of laboratory testing, and they are practically the same for each biomass species.

The structure and the particle size of the EMM ash depend on local technologies and the conditions of biomass preparation, and

Table 6
The OP 230 boiler calculation results for willow wood chips co-firing (boiler with no ash blowing).

Parameter	HC $Z_D = 0$	WWC_20 $Z_D = 0.2$
Max. continuous rating (t/h)	230	230
Steam pressure (MPa)	9.5	9.5
Feed water temperature (°C)	185	185
Spray water mass flow (kg/h)	18,270	20,268
Fuel		
Lower calorific value (kJ/kg)	21,034	19,511
Ash content (%)	22.69	17.59
Moisture content (%)	9.67	10.63
Steam temperatures (°C)		
At the superheater I stage (SH I) inlet	317	317
At the superheater III stage (SH III) outlet	540	540
Flue gas temperatures (°C)		
At the combustion chamber outlet	1230	1233
Before the economiser	538	551
Before the air preheater	349	359
At the boiler outlet	130	136
Air temperatures (°C)		
At the preheater inlet	25	25
At the preheater outlet	297	306
Boiler efficiency (%)	90.98	90.47
Fuel consumption (kg/h)		
HC	32,311	25,996
WWC	0	9036
Ash concentration in the ECO (g/m^3)	8.20	6.56
Flue gas velocity before the ECO (m/s)	6.22	6.54
c'_m index – formula (2) (–)	0.1129	0.1141
Mean fly ash diameter (μm)	45	45
Maximum annual erosion loss (mm/a)	0.0255	0.0239

these characteristics may not be defined in general terms. However, the EMM mixed with biomass may be coarse-grained and erosive (e.g., quartz sand), and thus its presence will increase the erosion hazard rather than tube fouling. Whenever biomass is put through coal mills, extra thick EMM grains may be ground. Therefore, laboratory testing of the granulation of the EMM (which can be separated from biomass mechanically) gives results that differ significantly from the grain distribution of the EMM fly ash (which, in practice, however, cannot be tested in the biomass co-fired boiler). Consequently, the only way to obtain a reliable evaluation of the $R_{0.03\Sigma}/R_{0.03W}$ ratio is to measure the particle size of the electrostatic precipitator ash for the combustion of coal only and for co-firing.

Yet, it is possible to apply the following type of reasoning to generalise the impact of co-firing on tube fouling; because the content of the IMM in the biomass plant matter is low and relatively constant and its ash also features very fine comminution, the smaller the biofuel value A^r is, the smaller the value of the $R_{0.03\Sigma}/R_{0.03W}$ ratio, and the stronger the tendency of the fly ash to form deposits on the boiler tubes of the heat exchangers more quickly. It may be assumed with a high probability that, for small values of A^r of the biomass, the ash is almost exclusively composed of the IMM. As the A^r value of the biomass increases, coarse EMM fractions may appear in the ash, and the rate of the fouling process may slow down.

Additionally, the fouling tendency is stronger when the share of co-fired biomass is higher (a higher share of fine particles in the coal-biomass ash mixture).

3.2. Ash blowing process

To perform a quantitative analysis of the impact of biomass co-firing on erosion resulting from the operation of ash blowers, appropriate calculations are performed for the OP 230 pulverised fuel boiler fired with hard coal.

The PS-SL blowers manufactured by the Clyde Bergemann company are used in the OP 230 boiler in the area of the banks of steam superheaters and economisers [26,27].

The Clyde-Bergemann PS-SL blowers mounted on the OP 230 boiler are referred to as long retractable sootblowers with an effective travel of 4.8 m (with blowing). The rate of the lance travel, extending and retracting, (1 blowing cycle) is $\tau_{c\,b} = 400$ s (velocity 24 mm/s). The blower takes in approximately 276 kg of steam per cycle. The blower lance makes a rotary motion during which the steam jets from two nozzles blow away the ash deposits on the tube banks. The steam outflow is parallel to the tubes of the heating surfaces because the blowers move perpendicularly to the tubes. The inside diameter of the blower lance is 42 mm. Each blower has 2 nozzles with a diameter of approximately 13.4 mm, which gives a total steam outflow area of $F_L = 0.00028$ m^2. The steam pressure is approximately 2 MPa. This type of pressure range involves a very high velocity of steam at the outlet of the nozzles.

The steam jet blower flow characteristics:

- steam mass flow

$$\dot{m}_{stb} = \frac{m_{stb}}{\tau_{cb}} = \frac{276}{400} = 0.69$$

(kg/s)

- lance section area $F_b = \frac{\pi d_b^2}{4} = \frac{\pi 0.042^2}{4} = 0.00139\ (\mathrm{m}^2)$
- superheated steam parameters at the blower inlet, $\left.\begin{array}{l} p = 20\ \mathrm{bar} \\ t = 400\ {}^\circ\mathrm{C} \end{array}\right\} i = 3248\ (\mathrm{kJ/kg}), \quad \rho = 6.61\ (\mathrm{kg/m^3}), \quad s = 7.13$ (kJ/kg K)
- steam flow velocity in the blower lance $w = \frac{\dot{m}_{stb}}{F_b \rho} = 75\ (\mathrm{m/s})$
- rest parameters of the superheated steam for isentropic change s = idem

$$i_0 = i + \frac{w^2}{2} = 3251\ (\mathrm{kJ/kg}) \Rightarrow t_0 = 401.5\ {}^\circ\mathrm{C}, \quad p_0 = 20.1\ \mathrm{bar}.$$

The equation of continuity implies that the maximum value, $(w\rho)$ = max, determined by means of a trial method and subject to the condition of constant entropy $s_0 = s_L$, occurs at the smallest cross-section of the nozzle. The calculation results are listed in Table 7. The steam velocity at the nozzle outlet is calculated according to the following dependence [28]:

$$w_L = \sqrt{2(i_0 - i_L)} \tag{8}$$

The superheated steam leaves the nozzle at a velocity close to $w_L = 600$ m/s at a pressure of $p_L = 10.8$ bar for a rest pressure of $p_0 = 20.1$ bar (Table 7).

The difference between the pressure forces in the smallest section and the ambient pressure forces results in an increase in the stream momentum and, consequently, in an increase in the jet velocity outside the nozzle to the value w_2.

Table 7
Characteristic steam parameters at the outlet of the steam jet blower nozzles.

p_L (bar)	i_L (°C)	ρ_L (kg/m^3)	w_L (m/s)	$w_L\rho_L$ (kg/m^{2}s)
15	3166	5.28	413.3	2187
12	3104	4.44	542.6	2411
11	3081	4.15	583.7	2426.4
10.9	3078	4.13	587.9	2426.8
10.8	3076	4.10	592.0	2626.4
10	3056	3.86	625.1	2414.0

$$w_2 = w_L + \frac{F_L}{\dot{m}_{stb}}(p_L - p_{ap})10^5 \tag{9}$$

If the pressure at the nozzle inlet is approximately 20 bar, the velocity resulting from expansion can reach values of up to 990 m/s. However, the jet of steam or air is slowed down rather abruptly at a short distance. The process is presented in Fig. 1 in relation to the air (perfect gas) flow for different values of the pressure [15]. Even after being slowed down by the start of the nozzles (the blower operation), the jet velocities are definitely higher than the velocity of the flow of dust-laden flue gases through the bank with shut down nozzles. The charts show that the higher the pressure before the nozzle, the higher the pressure after it. Thus, due to secondary expansion, the velocity of the gas agent in the area before the tube bank is also higher. The outermost tubes of the neighbouring stages of the steam superheaters between which the steam jet ash blower is installed are approximately 2 × 180 mm. Fig. 1 shows that the air jet velocity for $y = 180$ mm at a pressure of 31 bar is approximately 150 m/s, with a maximum velocity after secondary expansion of $w_2 = 580$ m/s. In the case of the steam jet blower, where the velocity is $w_2 = 990$ m/s after secondary expansion, the steam velocities before the tubes reach yet higher values. Therefore, for the analysis of the erosion caused by the temporary operation of the steam jet blower, the maximum values of the blowing agent are assumed to be at the levels of $w_{max} = 100$ m/s, $w_{max} = 150$ m/s, and $w_{max} = 200$ m/s.

The erosion rate $v_{e\,b}$ related to the use of blowers is unusually high, mainly due to the huge velocities given to the ash particles by the blowing agent. The factor that reduces the material loss is the relatively short annual time $\tau_{b\,a}$ of the duration of the process described above compared to the annual operating time of the boiler. Below, a calculation of time $\tau_{b\,a}$ is performed for the conditions prevailing in the area of the steam superheater and the economiser of the OP 230 boiler.

Based on the data concerning the blower operation characteristics, it is possible to determine the total annual time of the impact of the blower on the coils of the steam superheater and the economiser banks approximately:

- the number of starts per 24 h
  $n = 0$ for $Z_{D\ CWB} = 0\%$
  $n = 1$ for $Z_{D\ CWB} = 10\%$, $Z_{D\ CWB} = 20\%$, $Z_{D\ WWC} = 20\%$
  $n = 3$ for $Z_{D\ CWB} = 50\%$

- effective range of the blower$2 \times R = 240$ mm (assuming the distance from the bank tubes of approximately 180 mm [15])
- the travel rate $v_b = 24$ mm/s
- the unit time of the coil exposure to erosion during a single start of the blower making an extending and retracting movement $\tau_{b\,1} \cong 2 \times (2 \times R)/v_b = 20$ s

CWB represents the coniferous wood biomass, and WWC is the willow wood chips. The characteristics of both of these types of biomass are given in Section 1 of this paper.

If the blower is started three times per 24 h, which is considered the highest frequency used in practice, in a year (which, for the Polish power plants, corresponds to approximately $\tau_a \cong 6000$ h/a), the annual time of exposure is

$$\tau_{ba} = \frac{6000}{3600 v_b} n \tau_{bl} \cong (6000/(3600 \times 24)) \times 3 \times 20 \approx 4.2\ \mathrm{h/a}$$

If the blower is started only once, the time is $\tau_{b\,a} = 1.4$ h/a.

It may be assumed that the boiler banks are exposed to a more intense erosion for 1.4 (4.2) h of the 6000 h of operating time per year. Under these assumptions, the tube material loss according to formula (1) is the total of the loss without operating the blowers ($\tau_{nb\,a} = 5998.6$ h/a with the blower started once per 24 h, $\tau_{nb\,a} = 5995.8$ h with the blower started three times per 24 h) and the loss related to the blower operation for 1.4 or 4.2 h/a. Exemplary calculation results are listed in Tables 8 and 9.

The tables above show that, in each case, the tube material loss Δh, even when the steam jet blower operation is short, is greater than that during the entire rest of the time throughout a year when the blowers are shut down. In extreme cases, with a high content of biomass $Z_{D\ CWB} = 50\%$ and the blower operating time at the level of 4.2 h per year, the loss is greater than twice as large as that caused in the remaining 5995.8 h for $w_{max} = 200$ m/s.

The tube mass loss resulting from the blower operation is greater in the economiser (if the distance between the blower nozzles and the bank tubes is the same) than in the steam superheater despite the smaller mean velocities of the flue gases w_0 and due to the higher value of the parameter β_w that appears in formula (1) to the third power.

3.3. Conclusions

(a) The lower the ash content A^r in the co-fired biofuel and the higher the share of co-fired biomass, the more quickly the ash tends to settle on the boiler tubes of the heat exchangers. In such cases, both an increase in the amount of deposits and a decrease of the time in which the ash fouling accumulates to the maximum level are observed. Consequently, if the boiler is fitted with ash blowers, they are started more frequently; if not, they have to be installed.

(b) The operation of the jet blowers (using either air or steam) involves intense erosive wear of the cleared surfaces that suffer the erosion caused by fly ash, which is accelerated by the blowing jet. Despite the fact that the total time for which a cleared tube is exposed to the blower operation

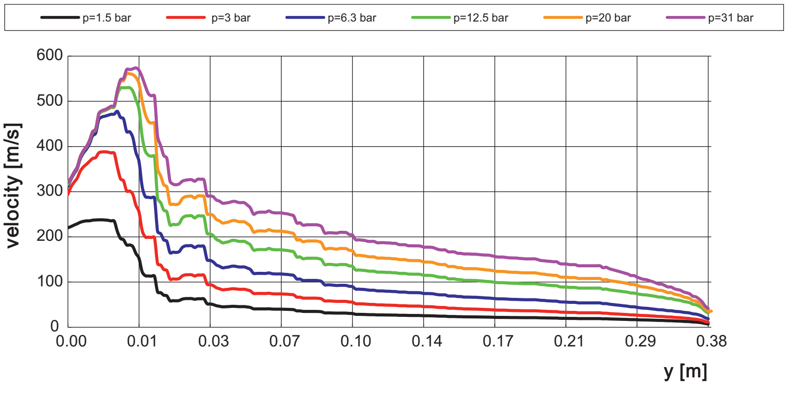

Fig. 1. Velocity distribution at the nozzle outlet depending on pressure.

Table 8
The material loss of the upper economiser tube throughout a year.

	$Z_{D\ CWB} = 0\%$		$Z_{D\ CWB} = 10\%$		$Z_{D\ CWB} = 20\%$		$Z_{D\ CWB} = 50\%$		$Z_{D\ WWC} = 20\%$	
Blower shut down $\beta_w = 1.4$										
	$\tau_{nb\ a} = 6000$ h		$\tau_{nb\ a} = 5998.6$ h		$\tau_{nb\ a} = 5998.6$ h		$\tau_{nb\ a} = 5995.8$ h		$\tau_{nb\ a} = 5998.6$ h	
	$w_0 = 6.22$ m/s		$w_0 = 6.74$ m/s		$w_0 = 7.27$ m/s		$w_0 = 8.92$ m/s		$w_0 = 6.54$ m/s	
	$n = 0$		$n = 1$		$n = 1$		$n = 3$		$n = 1$	
Δh (mm)	0.0255		0.034		0.0448		0.0965		0.0239	
Blower working $\beta_w = var$										
	$\tau_{b\ a} = 0$ h		$\tau_{b\ a} = 1.4$ h		$\tau_{b\ a} = 1.4$ h		$\tau_{b\ a} = 4.2$ h		$\tau_{b\ a} = 1.4$ h	
	$w_0 = 6.22$ m/s		$w_0 = 6.74$ m/s		$w_0 = 7.27$ m/s		$w_0 = 8.92$ m/s		$w_0 = 6.54$ m/s	
	β_w	Δh (mm)	β_w	Δh (mm)	β_w	Δh (mm)	β_w	Δh (mm)	β_w	Δh (mm)
w_{max} *(m/s)*										
100	–	0	14.84	0.0094	13.76	0.0099	11.21	0.0347	15.29	0.0073
150	–	0	22.26	0.0323	20.63	0.0335	16.82	0.1172	22.94	0.0245
200	–	0	29.67	0.0755	27.51	0.0793	22.42	0.2776	30.58	0.0581
$\Sigma\Delta h$ *(mm)*										
100	0.0255		0.0434		0.0547		0.1312		0.0312	
150	0.0255		0.0663		0.0783		0.2137		0.0484	
200	0.0255		0.1095		0.1241		0.3741		0.082	

Table 9
The material loss of the steam superheater tube throughout a year.

	$Z_{D\ CWB} = 0\%$		$Z_{D\ CWB} = 10\%$		$Z_{D\ CWB} = 20\%$		$Z_{D\ CWB} = 50\%$		$Z_{D\ WWC} = 20\%$	
Blower shut down $\beta_w = 1.4$										
	$\tau_{nb\ a} = 6000$ h		$\tau_{nb\ a} = 5998.6$ h		$\tau_{nb\ a} = 5998.6$ h		$\tau_{nb\ a} = 5995.8$ h		$\tau_{nb\ a} = 5998.6$ h	
	$w_0 = 9.24$ m/s		$w_0 = 9.9$ m/s		$w_0 = 10.57$ m/s		$w_0 = 12.57$ m/s		$w_0 = 9.65$ m/s	
	$n = 0$		$n = 1$		$n = 1$		$n = 3$		$n = 1$	
Δh (mm)	0.0528		0.0693		0.0897		0.1828		0.049	
Blower working $\beta_w = var$										
	$\tau_{b\ a} = 0$ h		$\tau_{b\ a} = 1.4$ h		$\tau_{b\ a} = 1.4$ h		$\tau_{b\ a} = 4.2$ h		$\tau_{b\ a} = 1.4$ h	
	$w_0 = 9.24$ m/s		$w_0 = 9.9$ m/s		$w_0 = 10.57$ m/s		$w_0 = 12.57$ m/s		$w_0 = 9.65$ m/s	
	β_w	Δh (mm)	β_w	Δh (mm)	β_w	Δh (mm)	β_w	Δh (mm)	β_w	Δh (mm)
w_{max} *(m/s)*										
100	–	0	10.1	0.0061	9.46	0.0065	7.96	0.0235	10.36	0.0046
150	–	0	15.15	0.0205	14.19	0.0218	11.93	0.0793	15.54	0.0156
200	–	0	20.2	0.0486	18.92	0.0517	15.91	0.188	20.73	0.0371
$\Sigma\Delta h$ *(mm)*										
100	0.0528		0.0754		0.0962		0.2063		0.0536	
150	0.0528		0.0898		0.1115		0.2621		0.0646	
200	0.0528		0.1179		0.1414		0.3708		0.0861	

amounts to a few hours per year only, the loss of the tube thickness in that period is higher than the loss caused during the overall remaining annual operating time of the boiler.

(c) It could be advantageous to replace the jet blowers with devices operating on a different principle that does not lead to erosion (such as the application of acoustic waves or microblasting technology).

References

[1] Rusin A, Wojaczek A. Influence of thermal loads variation on the probability of waterwall tubes corrosion failure in low-emission combustion. Rynek Energii 2009;6:129–33.

[2] Wejkowski R. CFD calculations for optimization of various air protection systems of evaporator tubes against low NO*x* corrosion (Wykorzystanie modelowania CFD do optymalizacji układów powietrza osłonowego chroniących kotły energetyczne przed korozją niskotlenową). Rynek Energii 2010;3(88) [in Polish].

[3] Pronobis M. Modernisation of power boilers. (Modernizacja kotłów energetycznych) WNT Warsaw; 2002 [in Polish].

[4] Foster DJ, Livingston WR, Wells J, Williamson J, Gibb WH, Bailey D. Particle impact erosion and abrasion wear – predictive methods and remedial measures. Report No. R241 DTI/Pub URN 04/701 – Mitsui Babcock (Internet).

[5] Raask E. Erosion wear in coal utilisation. Hemisphere Publishing Corporation; 1988. ISBN 3-540-18601-8.

[6] Kuzniecow N. Fly ash erosion and admissible flue gas velocities in boilers. Teploenergetika 1955/4. (Кузниецов Н.: Золовый износ труб и предельно допустимые скорости газов в котельных агрегатах. Теплоэнергетика 1955/4 [in Russian].

[7] Świrski J. Studies on ash erosion and the assessment of erosive wear of the boiler tubes caused by it. (Badania erozji popiołowej i ocena zużycia rur kotłowych wskutek jej działania) Prace Instytutu Energetyki, Book 1, Warsaw; 1975 [in Polish].

[8] Meuronen V. Ash particle erosion on steam boiler convective section. Lappeenranta University of Technology. Research Papers 64, Lappeenranta; 1997.

[9] Uetz H. Strahlverschleiß. Mitteilungen der VGB, Bd. 49, H. 1; 1969. p. 50–7.

[10] Fehndrich W. Verschleißuntersuchungen an Kesselrohren. Mitteilungen der VGB 1969;49:58–64.

[11] Parslow GI, Stephenson DJ, Strutt JE, Tetlow S. Paint layer erosion resistance behavior for use in a multilayer paint erosion indication technique. Wear 1997;212:103–9.

[12] Zhang L, Sazonov V, Kent J, Dixon T, Novozhilov V. Analysis of boiler-tube erosion by the technique of acoustic emission. Part I. Mechanical erosion. Wear 2001;250:762–9.

[13] Heiermann G, Langner H, Brinkmann C, Mondry H. Konstruktionskriterien zur erosionsminderung in wirbelschichtfeuerungen. wirbelschichtfeuerung und dampferzeugung, Essen; 1988.

[14] Raask E. Erosion durch aschepartikeln in kohlegefeuerten anlagen. VGB Kraftwerkstechnik 1979;59 H(6):496–502.

[15] Wojnar W. Identification of thermal and erosion hazards to reduce superheater failures (Identyfikacja zagrożeń termicznych i erozyjnych przegrzewaczy pary w celu zmniejszenia ich awaryjności). PhD thesis. Institute of Power Engineering and Turbomachinery, Silesian University of Technology, Gliwice; 2008 [in Polish].

[16] Schreier W, Schuster H. Feuerungssysteme für schwierige Kohlen. XXXII Kraftwerkstechnisches Kolloquium, Dresden; 2000.

[17] Pronobis M. Evaluation of the influence of biomass co-combustion on boiler furnace slagging by means of fusibility correlations. Biomass Bioenergy 2005;28(4):375–83.

[18] Pronobis M. The influence of biomass co-combustion on boiler fouling and efficiency. Fuel 2006;85:474–80.

[19] Kalisz S, Pronobis M, Baxter D. Co-firing of biomass waste derived syngas in coal power boiler. Energy 2008:1770–8.

[20] Kalisz S, Pronobis M. Investigations on fouling rate in convective bundles of coal fired boilers in relation to optimisation of sootblower operation. Fuel 2005;84(7–8):927–37.

[21] Test report 881/ZK/2008 – Ash from pine sawdust (Popiół z trocin sosnowych). IChPW, Zabrze; 1988 [in Polish].

[22] Pronobis M. Heat transfer in contaminated convection surfaces of boilers (Wymiana ciepła w zanieczyszczonych powierzchniach konwekcyjnych kotłów). Scientific Books of the Silesian University of Technology, series: Energetyka Gliwice (115); 1992 [in Polish].

[23] Basu P, Kefa C, Jestin L. Boilers and burners: design and theory. Springer; 2000.

[24] Hydrotech Systems Ltd.: The costs of air heater fouling; 1991.

[25] Test report 882/ZK/2008 – Ash from willow wood chips (Popiół ze zrębek wierzby). IChPW, Zabrze; 1988 [in Polish].

[26] Clyde Bergemann: company materials.

[27] Jameel M. Steam saving in recovery boilers. Bergemann USA, (Internet).

[28] Szargut J. The theory of thermal processes (Teoria procesów cieplnych). Warsaw: PWN; 1973 [in Polish].